ALOS Cal/Val Support at University of California San Diego: Radar Corner Reflectors for Interferometric Phase Assessment

David Sandwell[(1)], **Yuri Fialko**[(1)]

[(1)]University of California at San Diego, La Jolla, CA, USA, dsandwell@ucsd.edu

Abstract
We installed three radar corner reflectors at Pinon Flat Observatory located between the San Andreas and San Jacinto Faults to support the radiometric, geometric and interferometric assessment of PALSAR. The reflectors are permanent installations designed to remain in place for the lifetime of the ALOS mission and beyond. The precise locations of the reflectors and their radiometric design are available to any investigator. We have used 9 repeat swaths of PALSAR data over the reflectors to assess interferometric resolution, precision, and accuracy.

Keywords: radar reflector, geometric calibration

1. SAN ANDREAS FAULT AND REFLECTORS

The San Andreas Fault zone is a transform fault connecting the seafloor spreading ridges in the Gulf of California to the seafloor spreading on the Juan de Fuca Ridge off the Coast of Oregon. The metropolitan areas of San Francisco and Los Angeles lie along this transform fault and thus are at risk of a destructive Earthquake. Major earthquakes have occurred in 1906 in San Francisco and 1857 north of Los Angeles but a long section of the southern San Andreas Fault has remained locked for over 300 years so there is a concern that this will be the site of the next major rupture (Figure 1).

PALSAR aboard ALOS provided the first L-band radar interferograms of this tectonic area beginning in 2006. We participated in the ALOS calibration/validation phase of the mission by installing three radar corner reflectors at the Pinon Flat geodetic observatory (Figure 2 and Table 1). The reflectors are used for the geometric calibration of SAR imagery as well as assessment of interferometric phase. The reflectors have 2.4 m openings and are oriented at azimuths and elevations to provide optimal reflections of PALSAR on both descending and ascending tracks (Figure 2 and Table 1.).

2. INTERFEROMETRIC ASSESSMENT

The focus of our research has been on the assessment of the interferometric capabilities of ALOS PALSAR data in both FBS and FBD modes. In November of 2007 we submitted a paper on this topic to *IEEE Transactions on Geoscience and Remote Sensing***.** The title is: Accuracy and Resolution of ALOS Interferometry: Vector Deformation Maps of the Father's Day Intrusion at Kilauea. The authors are: David Sandwell, David Myer, Robert Mellors, Masanobu Shimada, Benjamin Brooks and James Foster. In addition to analyzing the interferometric capabilities of ALOS over Southern California, we also analyzed tens of interferograms over Hawaii to monitor crustal deformation at the Kilauea volcano, which has been very active recently. A shortened version of that manuscript follows.

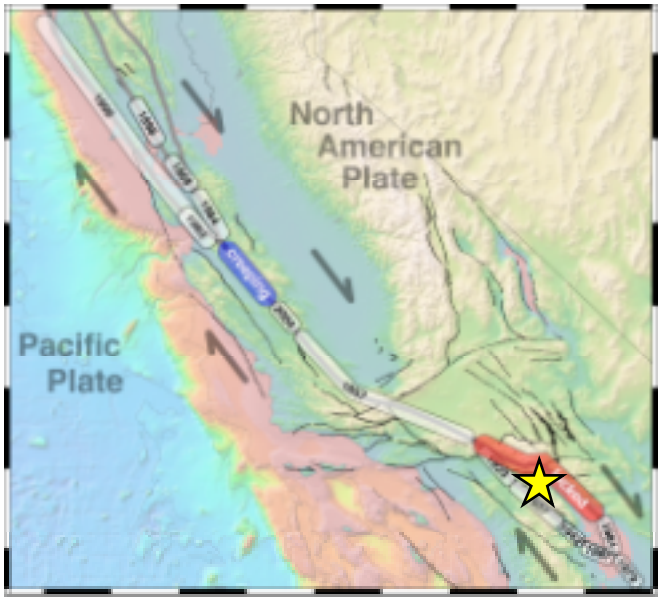

Figure 1. The major sections of the San Andreas Fault zone undergo repeated earthquake activity except along the creeping section where the plates slide smoothly at all depths. Recent major earthquakes are dominated by the 1857 Fort Tejon Earthquake (M7.9) and the 1906 San Francisco Earthquake (M8.3). The southernmost locked section of the San Andreas Fault has not experienced a major earthquake in at least 300 years. The next event along this section should release more than 7 m of accumulated slip; typically large California earthquakes have a maximum slip of 6 m. Pinon Flat Observatory (yellow star) lies hosts a wide array of geodetic and seismic instrumentation including three large radar corner reflectors.

We have been analyzing the accuracy, resolution, and coverage of the ALOS interferometry in preparation for geodetic imaging of the San Andreas Fault System (SAFS). This preliminary research has been funded by SIO, ConocoPhillips Corporation, and data generously provided

by JAXA through a calibration and validation effort, where we deployed three radar corner reflectors at Pinon Flat Observatory in southern California (Figure 3). Unlike most areas of the Earth where there are not yet more than 2-3 repeat radar images, JAXA has imaged the Pinon area on all flights (~45 times in 1.5 years). PALSAR data have been collected 9 times along an ascending track (T213), which contains sections of the San Jacinto, San Andreas, and Pinto Mountain faults (blue box in Figure 3). This area has more than 3000 m of relief, and includes forested and desert landscapes; images were acquired during both dry and snow-covered conditions. The area slightly to the east (green box in Figure 3) has been imaged 74 times at C-band wavelengths by ERS-1/2. These L- and C-band data are optimal for exploring the strengths and limitations of L- and C-band interferometry.

Figure 2. Photographs of one of the 3 radar reflectors. Reflectors D1 and D2 were installed at Pinon in 1997 were originally oriented to reflect radar from ERS-1 and ERS-2 having incidence angles of 23˚ and azimith of 102.5˚. In July of 2004 the reflectors D1 and D2 were adjusted to optimally reflect ALOS data with incidence angles between 34˚ and 43˚. In November of 2005 the ascending reflector was installed to reflector radar waves having an azimuth of 257.5˚ to reflect ALOS data along ascending passes.

Table 1. Coordinates of Radar Reflectors

position			orientation	
lat	lon	height	elev.	azi.
33.612246	-116.456768	1258.990	39˚	257.5˚
33.612253	-116.457893	1257.544	39˚	102.5˚
33.607373	-116.451836	1254.537	39˚	102.5˚

Latitude and longitude in decimal degrees and height in meters relative to the WGS-84 co-ordinate system and ellipsoid. The survey point is the apex (lowest corner) of each reflector. There should be a correction for the offset between the phase center of the reflector and the apex.

We expect that PALSAR has the duration and orbital accuracy needed to monitor slow crustal deformation globally [1, 2], although the revisit time of 46 days is rather long. The main advantages of the L-band (236 mm wavelength) PALSAR over C-band (56 mm wavelength) are: 1) less temporal decorrelation enabling interferograms having longer time separation [3]; and 2) a longer critical baseline resulting in more usable interferometric pairs (Table 2). The potential disadvantages are: 1) the lower fringe rate may results in less precise crustal motion measurements; and 2) the ionospheric refraction should be 16.5 times worse at L-band versus C-band. The path delays caused by water vapor in the troposphere are independent of wavelength, so this distortion will affect both systems equally [4].

In addition to these fundamental wavelength-dependent issues, PALSAR is operated in a number of different modes that could both enhance and detract from its interferometric capabilities [1]. In particular, the Fine Beam Single Polarization (FBS - HH, 28 MHz bandwidth) has 2 times better range resolution than most previous InSAR instruments, which further increases the critical baseline and could improve the spatial resolution of the interferograms. The Fine Beam Dual polarization (FBD - HH and HV, 14 MHz) has 2 times worse range resolution than the FBS mode. Table 2 shows the critical baseline, beyond which, phase coherence drops to zero. The orbits of ERS and ENVISAT are controlled within about a 1 km diameter tube, so not all pairs of SAR images can be used for interferometry because they commonly have baselines greater than the critical value [5]. Initially ALOS was controlled within about a 3 km tube, but since early 2007 the tube diameter has reduced to 1 km. Because the critical baseline for the typical PALSAR configuration is 6.5 or 13.1 km, every SAR pair can be used for interferometry.

Table 2. Comparison of critical baseline.

look angle	23˚	34˚	41˚
ERS/ENVISAT 16 MHz	1.1 km	2.0	2.9
ALOS FBD 14 MHz	3.6	6.5	9.6
ALOS FBS 28 MHz	7.3	13.1	18.6

ERS/ENVISAT: altitude = 790 km, wavelength = 56 mm; ALOS: altitude = 700 km, wavelength = 236 mm; Shaded area is most common mode for interferometry.

We used ALOS PALSAR data from the first 1.5 years of the mission to evaluate three quality parameters. First, we estimated the spatial resolution of the interferograms. This was done by cross-spectral analysis of independent interferograms. We computed interferograms from SAR image pairs having baselines of several hundred meters. The phase due to the topography of the Earth serves as a signal, which is common to both interferograms. The properly scaled difference of the two interferograms is a measure of the noise. The analysis of signal-to-noise ratio versus spatial wavelength provides an estimate of resolution in both range and azimuth directions. An identical analysis was performed using ERS interferometry [6], enabling a direct comparison of the resolution capabilities of ERS and ALOS. Second, we examined the amplitude of the phase

noise for the difference interferograms. To isolate the radar system noise from the atmospheric and orbital phase variations, we high-pass filtered the differenced interferograms for wavelengths shorter than 5 km and scaled the phase by the appropriate wavelength to form line-of-sight (LOS) difference maps. Finally, we assessed the overall accuracy of the ALOS InSAR system by constructing a vector deformation map associated with the June 17, 2007 (Father's Day) dike injection event at the Kilauea volcano, Hawaii. Nineteen continuous GPS stations within the interferograms provide ground truth deformation measurements. For all of these analyses, interferograms were constructed from images in the high bandwidth (FBS), low bandwidth (FBD), and mixed modes.

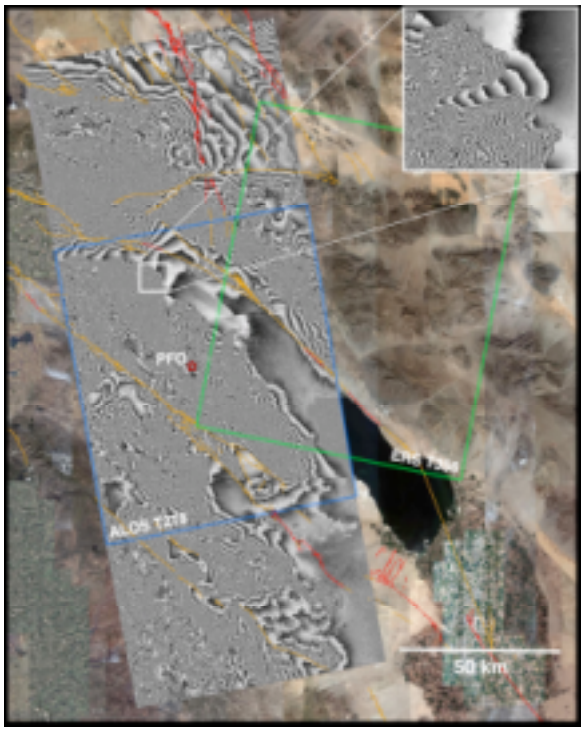

Figure 3. Example interferogram of the southern SAFS, near the Salton Sea, along ALOS track 213, frames 0650-0670 and look angle 34.3˚. The location of the Pinon Flat radar corner reflector is shown as a red star. The blue box marks the boundaries of track T213. JAXA has collected 9 repeat SAR swaths along this track during the past 1.5 years. A nearby ERS scene (T356), where 74 repeats are available, is marked by the green box. Red lines mark currently active faults and the yellow lines are active faults that have not ruptured in historical times. The inset box shows the high fringe rate associated with the 3000 m of relief in the area. One fringe corresponds to 86 m of elevation change.

The primary conclusions of this analysis follow:

(1) *Baseline decorrelation* - The critical baseline of ALOS is 6.5 km for the FBD2FBD interferometry and 13 km for the FBS2FBS interferometry. None of our possible interferometric baselines exceeded 3 km and newer data have baselines less than 0.5 km. Therefore, baseline decorrelation is not an issue with ALOS. Moderate baseline (~1 km) ALOS interferograms could be used to improve the accuracy of SRTM topography.

(2) *Spatial resolution* - Using topography as a common signal in independent interferograms, we find that the best spatial resolution (1/4 wavelength) achievable with ALOS is 38 m in range and 30 m in azimuth. This is slightly better than the resolution from Tandem ERS interferometry (57 m and 45 m, respectively). The improvement in ALOS is due to its longer critical baseline. We do not find any significant differences in spatial resolution between the FBF2FBS, FBS2FBD, and FBD2FBD interferograms and note that our test interferograms had baselines less than 10% of the critical baseline.

(3) *Radar noise* - Simple wavelength scaling arguments predict that the LOS range precision of L-band interferometry should be 4 times worse than C-band interferometry. These arguments are incorrect in the case of ALOS PALSAR, where we find that LOS range precision of ALOS is only 1.5 times worse than ERS (3.3 mm vs. 2.1 mm). In both cases, the largest source of error is tropospheric phase delay.

(4) *Overall accuracy* - The June 17, 2007 rift event at Kilauea provides an optimal signal for assessing the overall accuracy of ALOS interferometry (Figure 4). Comparisons of 19 GPS vectors projected into the LOS of the ascending and descending interferograms show an RMS deviation of 14 mm. The surprising result is that the azimuth offsets show a standard deviation of 71 mm. This is a remarkable result considering 71 mm is only 2% of the azimuth pixel size. The high precision of the azimuth offsets could be due to a combination of increased aperture length and low phase noise. The implication is that 4 components of displacements can be extracted from just two interferograms when the signal is large (> 200 mm) and the coherence is high.

(5) *Atmosphere and ionosphere errors* - As expected, we observe phase errors that are probably due to tropospheric water vapor. Ionospheric errors should be 16 times worse at L-band wavelengths and we have not assessed the longer wavelength ionosphere and orbital errors in this analysis [7, 8].

(6) *Temporal decorrelation* - Although we have not yet performed a systematic study of temporal decorrelation, we have analyzed ALOS data from a variety of surfaces, including jungles in Venezuela and Hawaii, as well as snow-covered regions in Canada. In our analysis of ~100 interferograms, we have not found any interferometric pairs having low coherence except for the areas of deep snow cover in Canada. We have been able to unwrap the phase of all cases (except Canada) using the standard Goldstein algorithm [9].

This resolution/accuracy analysis of ALOS interferometry was used to optimize our InSAR processing methods in preparation for a more extensive analysis. A preprocessor for ALOS L1.0 raw SAR data has been developed by R. Mellors (San Diego State University) and D. Sandwell and

is available at the UNAVCO WInSAR website (http://winsar.unavco.org). This includes code to 1) align the radar echoes to a common rear range and extract parameters for focusing the imagery (ALOS_pre_process); 2) merge raw SAR files from adjacent frames (ALOS_merge); 3) calculate interferometric baselines (ALOS_baseline); and 4) convert between the FBS and FBD modes (ALOS_fbd2fbs). This preprocessor has been installed in ROI_PAC by Yuri Fialko (UC San Diego) and Eric Fielding (Jet Propulsion Laboratory); these scripts are also available at the UNAVCO WInSAR site. In addition, we have implemented other capabilities in our in-house InSAR system (SIOSAR freely available but not supported) to handle varying pulse repetition frequencies, as well as the elevation-dependent range shifts associated with long baseline interferograms (> 1000 m).

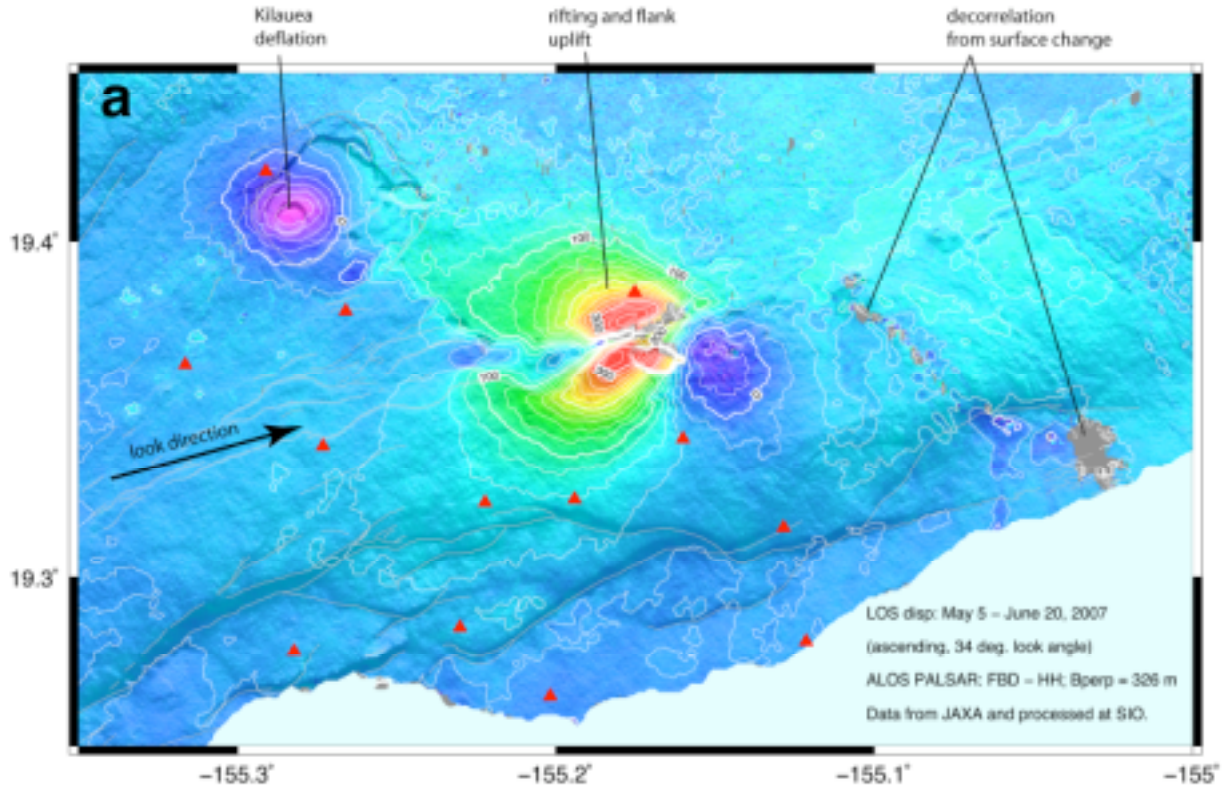

Figure 4. Line-of-sight (LOS) displacement (mm) from radar interferograms constructed from ALOS PALSAR acquisitions on May 5 and June 20, 2007. This time period spans most of the "Fathers Day" (June 17-20) rift event. These data were acquired in the fine beam dual polarization mode (FBD-HH, 14 MHz). Correlation is high, even in forested areas, and the phase was unwrapped and scaled LOS millimeters. The radar look direction is from the WSW and 34° from vertical. GPS receivers with continuous vector measurements are marked by red triangles. More complete ALOS interferometric analysis of this event can be found at http://topex.ucsd.edu/kilauea.

3. REFERENCES

[1] Shimada, M., et al. PALSAR CALVAL Summary and Update 2007. in IGARSS07. 2007. Barcelona, Spain: *IEEE Trans. Remote Sensing*.

[2] Rosenqvist, A., et al., ALOS PALSAR: A Pathfinder Mission for Global-Scale Monitoring of the Environment. *IEEE Trans. Geos. Remote Sens*., 2007. 45: p. 1-20.

[3] Rosen, P.A., et al., Surface deformation and coherence measurements of Kilauea Volcano, Hawaii from SIR-C radar interferometry. *J. Geophys. Res.*, 1996. 101(E10): p. 23109-23125.

[4] Hanssen, R.F., *Radar Interferometry: Data Interpretation and Error Analysis*. 2001, Boston: Dordrecht: Kluwer Academic Publishers. 308 pp.

[5] Massonnet, D. and K. Feigl, Radar Interferometry and its Application to Changes in the Earth's Surface. *Reviews of Geophysics*, 1998. 36(4): p. 441 - 500.

[6] Sandwell, D.T. and E.J. Price, Phase gradient approach to stacking interferograms. *J. Geophys. Res.,* 1998. 103(B12): p. 30183-30204.

[7] Tarayre, H. and D. Massonnet, Atmospheric propagation heterogeneities revealed by ERS-1 interferometry. *Geophys. Res. Lett.,* 1996. 23: p. 989-992.

[8] Xu, Z.W., J. Wu, and Z.S. Wu, A survey of ionospheric effects on space-based radar. *Waves in Random Media*, 2004. 14: p. S189-S273.

[9] Goldstein, R.M., H.A. Zebker, and C. Werner, Satellite radar interferometry - Two-dimensional phase unwrapping. *Radio Science*, 1998. 23: p. 713-720.